

Ground state and thermal transitions in Field Induced spin-Supersolid Phase

P. Sengupta^{1,2} and C. D. Batista¹

¹Theoretical Division, Los Alamos National Laboratory, Los Alamos, NM 87545

²MPA-NHMFL, Los Alamos National Laboratory, Los Alamos, NM 87545

(Dated: December 1, 2018)

We use a quantum Monte Carlo method to study the ground state and thermodynamic phase transitions of the spin supersolid phase in the $S = 1$ Heisenberg model with uniaxial anisotropy. The thermal melting of the supersolid phase shows unique signatures in experimentally measurable observables. This Hamiltonian is a particular case of a more general and ubiquitous model that describes the low energy spectrum of a class of *isotropic* and *frustrated* spin systems. We also discuss some alternative realizations of spin supersolid states in real magnets.

PACS numbers: 75.10.Jm, 75.40.Mg, 75.40.Cx

The supersolid (SS) state of matter has attracted great interest lately following the experiments of Kim and Chan on solid ^4He . While it is still unclear whether it can be stabilized in the continuum, there are several numerical studies which show that a SS phase can be realized in the presence of a periodic potential or underlying lattice for bosons [2, 3, 4] as well as spins [5, 6]. The SS state is easier to stabilize on a lattice because the lattice parameter of the “solid phase” or charge density wave cannot relax to any arbitrary value (it has to be an integer multiple of the underlying lattice parameter). In this work we have studied a class of spin-SS on cubic lattices, focusing primarily on the unique signatures of the thermal melting of the SS in experimentally measurable observables. We also discuss different conditions under which a spin-SS can be realized in real spin compounds.

The minimal spin model that has a thermodynamically stable supersolid ground state on a bipartite lattice is the $S = 1$ Heisenberg model with uniaxial single-ion and exchange anisotropies and an external magnetic field:

$$H_H = J \sum_{\langle \mathbf{i}, \mathbf{j} \rangle} (S_i^x S_j^x + S_i^y S_j^y + \Delta S_i^z S_j^z) + \sum_{\mathbf{i}} (D S_i^{z2} - B S_i^z) \quad (1)$$

where $\langle \mathbf{i}, \mathbf{j} \rangle$ indicates that \mathbf{i} and \mathbf{j} are nearest neighbor sites, D is the amplitude of the single ion-anisotropy and Δ determines the magnitude of the exchange uniaxial anisotropy. Note that although the exchange interaction is anisotropic, the longitudinal (J) and transverse (Δ) couplings are both AFM (positive). Henceforth, J is set to unity and all the parameters are expressed in units of J .

The ground state properties of the above model on a square lattice were studied in detail previously [6]. For $D, \Delta > 1$, the ground state is supersolid over a finite range of applied field B . In this work, we report the ground state and thermodynamic properties of (1) on a cubic lattice. While the quantum phase diagram remains qualitatively unchanged, the thermodynamic properties are different in three dimensions (3Ds) because the condensate (XY ordered antiferromagnetic phase) extends to finite temperatures. Additionally, the melting of this phase belongs to the XY universality class as opposed to Kosterlitz-Thouless (KT) type in two dimensions (2Ds). This

has important consequences in any putative experimental detection of the SS phase, as we shall discuss below.

The Stochastic Series expansion (SSE) quantum Monte Carlo (QMC) method [7] is used to study the Hamiltonian (1) on cubic lattices $N = L \times L \times L/2$, with $8 \leq L \leq 16$. To characterize the different phases, we compute the longitudinal component of the staggered static structure factor (SSSF),

$$S^{zz}(\mathbf{Q}) = \frac{1}{N} \sum_{j,k} e^{-i\mathbf{q} \cdot (\mathbf{r}_j - \mathbf{r}_k)} \langle S_j^z S_k^z \rangle, \quad \mathbf{Q} = (\pi, \pi, \pi), \quad (2)$$

and the spin stiffness, ρ_s , defined as the response of the system to a twist in the boundary conditions. $S^{zz}(\mathbf{Q})$ measures the extent of diagonal (Ising like) long-range order (LRO) at the ordering wave vector $\mathbf{Q} = (\pi, \pi, \pi)$, while the stiffness (superfluid density in particle language [8]), indicates the presence of XY (off-diagonal) LRO (this is not true for $D < 3$). In 3D, the superfluid density is identical to the condensate fraction. In the simulations, the stiffness is obtained from the winding numbers of the world lines along the three axes: $\rho_s = \langle W_x^2 + W_y^2 + W_z^2 \rangle / 3\beta$ [9].

Ground state (GS) phases As the field, B , is varied, the GS of (1) goes through a succession of phases, including spin-gapped Ising-ordered (IS) and gapless XY-ordered (XY) states. The IS phase is marked by a diverging value of $S^{zz}(\mathbf{Q}) \propto N$ in the thermodynamic limit, whereas a finite ρ_s characterizes the gapless XY ordered phase. A spin SS phase is identified by a finite value of both $S^{zz}(\mathbf{Q})/N$ and ρ_s [10]. Both quantities are always finite for finite size systems and estimates for $N \rightarrow \infty$ are obtained from finite-size scaling.

Fig. 1 shows the quantum phase diagram as a function of magnetic field, B , for $D = 3.0$ and $\Delta = 6.0$ – it is qualitatively similar to that obtained in 2Ds [6]. The $m_z(B)$ curve features two prominent plateaus corresponding to different IS phases. For small B , the GS is a gapped AFM solid (IS1) with no net magnetization. The stiffness, ρ_s , vanishes in the thermodynamic limit, while $S^{zz}(\mathbf{Q})/N \approx 1$ with the spins primarily in the $S_i^z = \pm 1$ states in the two sublattices. At a critical field, B_{c1} , there is a second order transition to a state with a finite fraction of spins in the $S_i^z = 0$ state. These

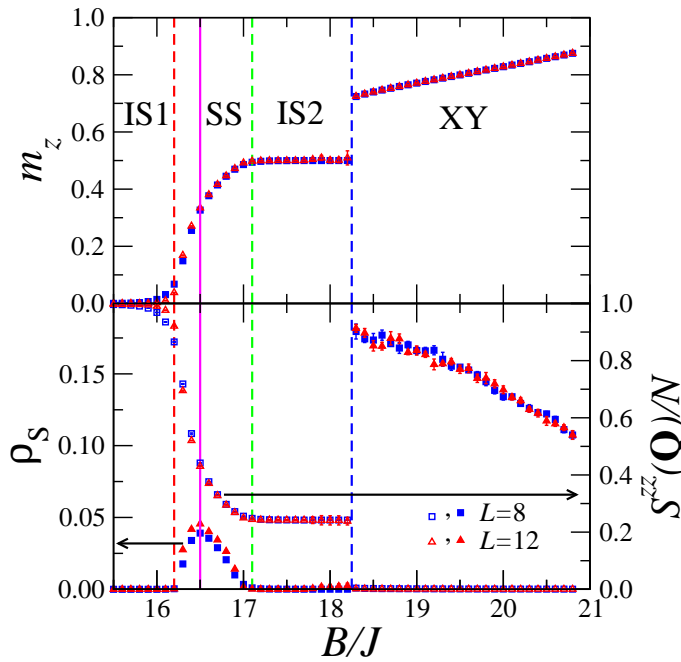


FIG. 1: (Color online) Quantum phase diagram of H_H (Eq. 1) for $D = 3.0$ and $\Delta = 6.0$. The upper panel shows the magnetization as a function of field B . The SS phase appears between the two Ising-like phases IS1 and IS2. At higher fields, there is a first order transition to a pure XY-AFM phase. The lower panel shows the stiffness and the longitudinal component of the SSF. The SS phase has finite values of both observables.

$S^z = 0$ “particles” Bose-Einstein condense (BEC) to give the GS a finite stiffness. The diagonal order is reduced but remains finite as well. The resulting GS thus has simultaneous long-range diagonal and off-diagonal order; in other words, it is a spin-supersolid. The complete phase diagram consists of a second gapped Ising phase (IS2) with diagonal order (all the spins in the $S^z = -1$ sublattice are flipped to $S^z = 0$) and an XY phase at very high fields with pure off-diagonal ordering.

Finite temperature transitions Finite temperature properties of the SS has previously been examined for hard core bosons[3, 11, 12] and $S = \frac{1}{2}$ spins on a bilayer[13]. The melting of the SS phase proceeds via two steps – the superfluid order disappears at a lower temperature whereas the solid order persists up to a higher temperature. In 2Ds, the continuous U(1) symmetry cannot be broken at $T > 0$ and the SS has only a quasi long-range off-diagonal order for $T < T_{KT}$. The vanishing of the spin stiffness occurs via a KT transition. In contrast, true long-range off-diagonal order in the SS persists to finite temperatures in 3Ds and the melting of the superfluid order belongs to the XY universality class. The solid order disappears at a higher temperature via an Ising-like transition.

The results of simulations of thermal transitions associated with the SS phase are shown in fig.2. The top panel shows the variation of the solid and superfluid order parameters as a function of temperature. At low temperatures, both order parameters are finite. With increasing T , the SS “melts” into

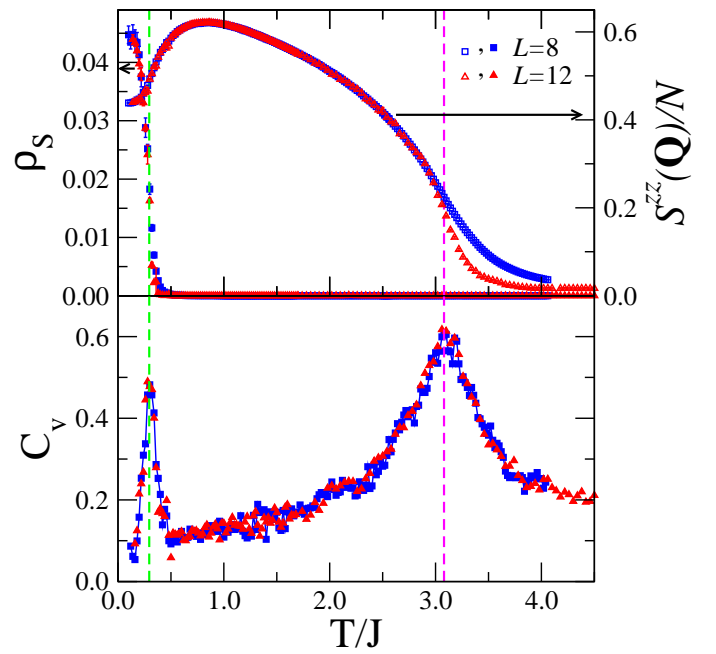


FIG. 2: (Color online) Two-step melting of the SS for parameters in Fig.1 and $B/J=16.5$ (solid line in Fig.1). The top panel shows the vanishing of the two orders at different temperatures. The disappearance of superfluidity is accompanied by an unusual increase in the solid order parameter. The lower panel shows the signatures in the specific heat at the two transitions.

a pure solid. The disappearance of SF order is marked by an enhancement in the solid order. This apparently anomalous behavior reflects the fact that in the SS phase, the solid order is partially suppressed by the co-existing SF order. The longitudinal component of the SSF is accessible experimentally by neutron scattering and its non-monotonic behavior at the onset of superfluid order can serve as an important signature of the SS phase. The three dimensionality of the model implies that the two transitions should be accompanied by specific heat anomalies at the corresponding temperatures. The XY transition will manifest itself as a λ -anomaly while the Ising-like solid melting will be marked by a cusp. Indeed we find clear signatures of the two transitions in the calculated specific heat (lower panel of fig.2). While both the peaks are rounded by finite-size effects, their positions coincide unambiguously with the melting of the superfluid and Ising orders. Since it is one of the most readily measurable observables, having clear signatures in the specific heat is of great experimental relevance.

Next we discuss the relevance of these results for finding a SS phase in real magnets. The magnetic properties of spin compounds with spin-orbit interaction much smaller than the crystal field splitting can be adequately described by a U(1) invariant model (although this invariance is never perfect)[10]. The transition metal magnetic ions belong to this class. On the other hand, the exchange anisotropy is typically very small in these compounds. The above model with large Δ is not di-

rectly applicable to this class of real quantum magnets. We shall show below that under appropriate conditions, an effective uniaxial exchange anisotropy can be generated in the low-energy subspace of a model with (realistic) isotropic interactions. To this end we consider coupled layers of dimers with only *isotropic* (Heisenberg) AFM interactions – an intra-dimer exchange J_0 and weaker inter-dimer *frustrated* couplings J_1 and J_2 (see Figs. 3(a) and 3(b)):

$$H_D = J_0 \sum_i \mathbf{S}_{i+} \cdot \mathbf{S}_{i-} + J_1 \sum_{(i,j),\alpha} \mathbf{S}_{i\alpha} \cdot \mathbf{S}_{j\alpha} + J_2 \sum_{(i,j),\alpha} \mathbf{S}_{i\alpha} \cdot \mathbf{S}_{j\bar{\alpha}} - B \sum_{i\alpha} S_{i\alpha}^z. \quad (3)$$

The index $\alpha = \pm$ denotes the two spins on each dimer.

For $S = 1$ dimers, the low energy subspace of H_D (for $J_1, J_2 \ll J_0$) consists of the singlet, the $S^z = 1$ triplet and the $S^z = 2$ quintuplet (see Fig. 3(a)). The low energy effective model that results from restricting H_D to this subspace supports a field-induced supersolid phase on a bipartite lattice for $J_0 > z(J_1 + J_2)/2$ and $J_0 \gg z(J_1 - J_2)/2$ (z is the co-ordination number of the lattice) as was shown in Ref.[6].

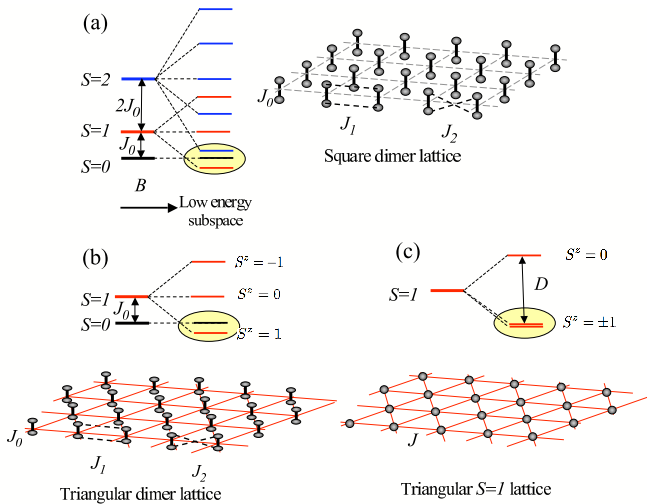


FIG. 3: (Color online) (a) Square lattice of $S=1$ dimers with an intra-dimer Heisenberg AFM interaction J_0 and inter-dimer interactions J_1 and J_2 . The level diagram shows the low energy subspace of the single dimer spectrum in the presence of a magnetic field. (b) $S = 1/2$ dimers on a triangular lattice and the low energy subspace of a single dimer. (c) $S = 1$ spins on a triangular lattice and the energy level splitting for easy-axis single-ion anisotropy.

For $S = 1/2$ dimers the low energy subspace of H_D consists of the singlet and the $S^z = 1$ triplet states in the limit $J_0 \ll J_1, J_2$ (see Fig. 3(b)). The resulting low-energy effective model is a $t - V$ Hamiltonian for hard core bosons:

$$H_{eff} = -t \sum_{(i,j)} (b_i^\dagger b_j + b_j^\dagger b_i) + V \sum_{(i,j)} n_i n_j - \mu \sum_i n_i \quad (4)$$

b_i^\dagger creates a $S^z = 1$ triplet state at site i whereas the singlet corresponds to the empty boson state; n_i is the boson number

operator $b_i^\dagger b_i$ and the parameters of the effective model are expressed in terms of those of the original Hamiltonian H_D as $t = (J_1 - J_2)/2$, $V = (J_1 + J_2)/2$ and $\mu = -J_0 + B$. On many frustrated lattices, this model contains a SS phase in its quantum phase diagram for $t < 0$ and $V \gg |t|$ [3, 4, 12]. In terms of the original model, this implies that $S = 1/2$ dimers with frustrated inter-dimer couplings, $J_2 \gtrsim J_1$ provides an alternative realization of a spin-SS on different frustrated lattices.

As a final example, we consider $S = 1$ Heisenberg model with large easy-plane single-ion anisotropy ($\Delta = 1$ and $D < 0$ in Eq.(1)). For $|D| \gg J$ the low-energy subspace consists of the $S_i^z = \pm 1$ states (see Fig. 3(c)). The low-energy effective model is once again the $t - V$ Hamiltonian (4) with $t = -J^2/2D$, $V = J + J^2/D$ and $\mu = B - J^2/D - 2n_b J$, up to second order in J/D . n_b is the number of bonds per site. As in the previous case, a SS phase is realized for $V \gg |t|$ on different frustrated lattices[3, 4, 12]. The BEC component corresponds to spin nematic ordering.

In conclusion, we have used numerical simulation to study the ground state and thermodynamic phase transitions involving the spin-supersolid phase in a $S = 1$ Heisenberg model with uniaxial exchange and single-ion anisotropies on a cubic lattice. The melting of the SS occurs in two steps with the XY and Ising ordering disappearing at different temperatures. The transitions are marked by unique features in the structure factor and the specific heat which will be useful in any experimental detection of the SS. Finally, we discuss several different conditions under which a SS can be realized in real spin compounds.

LANL is supported by US DOE under Contract No. W-7405-ENG-36.

- [1] E. Kim and M. H. W. Chan, Nature **427** 225 (2004); Science **305**, 1941 (2004).
- [2] P. Sengupta *et al*, Phys. Rev. Lett. **94**, 207202 (2005).
- [3] M. Boninsegni and N. Prokof'ev, Phys. Rev. Lett. **95**, 237204 (2005).
- [4] S. Wessel and M. Troyer, Phys. Rev. Lett **95**, 127205 (2005); D. Heidarian and K. Damle *ibid* **95**, 127206 (2005); R. G. Melko *et al.*, *ibid* **95** 127207 (2005).
- [5] K-K Ng and T. K. Lee, Phys. Rev. Lett. **97**, 127204 (2006).
- [6] P. Sengupta and C. D. Batista, Phys. Rev. Lett. **98**, 227201 (2007).
- [7] A. W. Sandvik, Phys. Rev. B **59**, 14157(R), (1999).
- [8] C. D. Batista and G. Ortiz, Phys. Rev. Lett. **86**, 1082 (2000); Adv. **53**, 1 (2004).
- [9] E. M. Pollock and D. M. Ceperley, Phys. Rev. B **36**, 8343, (1987).
- [10] In real systems, spin-orbit interactions will remove the finite stiffness by opening a gap in the excitation spectrum. However, the U(1)-invariant model considered here provides a very good description of the static properties of real systems as long as the temperature is higher than the the small U(1)-symmetry breaking terms.
- [11] G. Schmid and M. Troyer, Phys. Rev. Lett. **93**, 67003 (2004).

- [12] T. Suzuki and N. Kawashima, Phys. Rev. B **75**, 180502(R), (2007). [13] N. Laflorencie and F. Mila, Phys. Rev. Lett. **99**, 27202 (2007).